

# PROCEEDINGS OF SPIE

[SPIEDigitalLibrary.org/conference-proceedings-of-spie](https://SPIEDigitalLibrary.org/conference-proceedings-of-spie)

## Cavitation bubbles induced by Erbium lasers: implications for dentistry

Marja Verleng, Rudolf Verdaasdonk, Albert van der Veen, Vladimir Lemberg, Dmitri Boutoussov

Marja Verleng, Rudolf Verdaasdonk, Albert van der Veen, Vladimir Lemberg, Dmitri Boutoussov, "Cavitation bubbles induced by Erbium lasers: implications for dentistry", Proc. SPIE 8929, Lasers in Dentistry XX, 89290B (18 February 2014); doi: 10.1117/12.2039282

**SPIE.**

Event: SPIE BiOS, 2014, San Francisco, California, United States

# Cavitation bubbles induced by Erbium lasers: implications for dentistry

Marja Verleng<sup>a</sup>, Rudolf Verdaasdonk<sup>a</sup>, Albert van der Veen<sup>a</sup>,  
Vladimir Lemberg<sup>b</sup>, Dmitri Boutoussov<sup>b</sup>

<sup>a</sup> VU University Medical Center, Dept. Physics & Med Technology,  
PO Box 7057, 1007 MB Amsterdam, The Netherlands;

<sup>b</sup> Biolase Inc, Irvine, CA, USA

Contact: r.verdaasdonk@vumc.nl

## ABSTRACT

With new fiber systems available for 3  $\mu\text{m}$ , Erbium lasers become more interesting for precise tissue ablation in a water environment enabling new application in e.g. dentistry. The dynamics of explosive bubble formation was investigated at 2.78  $\mu\text{m}$  (Er,Cr;YSGG) and 2.94  $\mu\text{m}$  (Er:YAG), in relation to energy (10-50 mJ), pulse length (20–150  $\mu\text{s}$ ) and fiber tip shape (flat or taper). The dynamics of exploding and imploding vapor bubbles were captured with high speed imaging (10 - 300  $\mu\text{s}$  range). Increasing the pulse length and energy, the vapor bubble became more elongated with an opaque surface for flat tip fibers. Tapered fibers produced spherical vapor bubbles with an optically transparent surface expected to be more forceful for creating mechanical effects in both hard and soft tissues. There was no significant difference between bubbles formed at 2.78  $\mu\text{m}$  (Er,Cr;YSGG) and 2.94  $\mu\text{m}$  (Er:YAG).

**Keywords:** Erbium laser, Er,Cr;YSGG, Er:YAG, high speed imaging, explosive vapor bubble, cavitation

## 1. INTRODUCTION

Cavitation is a phenomenon where cavities are formed in a liquid and implode within a short time ( $\mu\text{s}$  range). Cavitation bubbles can be induced in various ways, for example through the use of short laser pulses. The implosion of a cavitation bubble creates forceful local stresses which can be applied in various medical procedures [1]. Extracorporeal generated shockwaves were first used in medicine about 30 years ago, as a treatment method for fragmentation of kidney stones. Since then, the method has evolved as treatment modality in many more medical fields, such as urology, orthopedics, cardiology, dermatology and dentistry [2].

The focus of this study is the dynamics of explosive bubble formation and implosion (cavitation) induced by Erbium lasers. Erbium lasers are mostly used in dermatology and dentistry for either superficial and precise ablation of soft tissue or hard tissue cutting. With new fiber systems becoming available to transmit wavelengths around 3  $\mu\text{m}$ , there is a growing interest in the usage of Erbium lasers in a water environment like urology, ENT, neurosurgery and applications in dentistry. In dentistry, laser-induced cavitation can be used e.g. to clean and sterilize root canals. A thin fiber tip is moved up and down inside a root canal, which has been filled with water. An artist impression of such a procedure is shown in figure 1.

However, little is known about the exact characteristics of the dynamics of cavitation created by these lasers. In this study, the dynamics of explosive bubble formation in water are investigated in relation to absorption at 2.78  $\mu\text{m}$  (Er,Cr;YSGG) and 2.94  $\mu\text{m}$  (Er:YAG), with various pulse lengths and fiber tip shapes. Using time delayed high speed  $\mu\text{s}$  flash imaging, sequences of the dynamics of exploding and imploding bubbles between 10 and 300  $\mu\text{s}$  are assembled for various pulse energies. The characteristic shape and size of the bubbles are determined in relation to time.

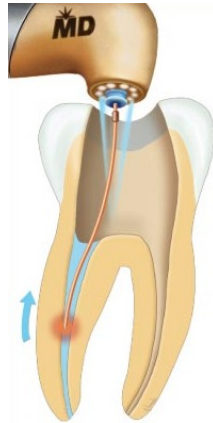


Figure 1. Illustration of the cleaning of a root canal using laser-induced cavitation. Image from [www.biolase.com](http://www.biolase.com)

## 2. THEORY

### 2.1 Laser systems and wavelengths

The laser systems used in this study are the Erbium, Chromium-doped:Yttrium, Scandium, Gallium, Garnet (Er,Cr:YSGG) laser, and the Erbium-doped: Yttrium, Aluminum, Garnet (Er:YAG) laser (both Waterlase Millennium, Biolase, Irvine, Ca, USA). These lasers are optically pumped flash lamp solid-state lasers [4]. The laser light has a wavelength of 2.78  $\mu\text{m}$  and 2.94  $\mu\text{m}$  for the Er,Cr:YSGG laser and Er:YAG laser, respectively. These wavelengths are highly absorbed by water (see figure 2) which causes an instant vaporization of the water surrounding the laser tip. This makes Erbium lasers an interesting tool for medical procedures in watery environments.

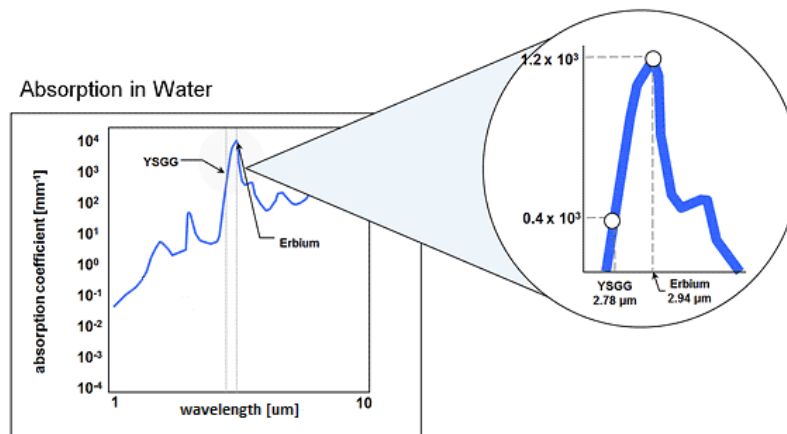


Figure 2. Absorption in water by wavelength for Er,Cr:YSGG (YSGG) and Er:YAG (Erbium) lasers. Adapted from [www.biolase.com](http://www.biolase.com)

### 2.2 Laser-tissue interactive of Erbium lasers

During the laser pulse, water is vaporized creating a (vapor) cavity in the water. When the laser pulse ends, this cavity implodes due to vapor condensation and outer water pressure, which can create a shockwave at the center point of the implosion.

Historically, interest in cavitation began when its destructive effect on solid surfaces such as ship propellers became apparent. Cavitation bubbles have been studied using different techniques. A theory of the collapse of spherical cavitation bubbles was first given by Rayleigh (1917). He found that the time needed for each collapse is related to its maximum radius. He derived the relationship [4] :

$$r_{max} = \frac{t_c}{0.915 \sqrt{\rho / (p_{stat} - p_{vap})}} \quad (1)$$

Where  $r_{max}$  is the maximum radius of cavitation,  $t_c$  is the duration of the collapse,  $\rho$  is the density of the fluid,  $p_{stat}$  is the static pressure and  $p_{vap}$  is the vapor pressure of the fluid. Furthermore, the maximum radius of the bubble is related the bubble energy,  $E_b$  .

Rayleigh found the following relation [4] :

$$E_b = 4/3 \pi (p_{stat} - p_{vap}) r_{max}^3 \quad (2)$$

The high absorption coefficients of Erbium lasers in water result in very short penetration depths of around 10  $\mu$ m. For a 200  $\mu$ m, flat fiber tip, less than 1 mJ is needed to start vaporization of water in front of the tip.

### 2.3 Beam characteristics

The transmission of the 2.78 and 2.94  $\mu$ m Erbium wavelengths through normal optical fibers is very low. The loss is in the range of 800 dB per meter [5]. Therefore, the laser light is transmitted through a hollow waveguide for most part with a loss in the range of 1 dB per meter [6]. The hollow waveguide ends in hand piece and only for the very last part, the beam is transmitted through a short fiber tip made of sapphire or silica with high but acceptable energy loss. An example of a dental hand piece with a laser tip is shown in figure 3.



Figure 3. A dental hand piece with fiber tip.  
Image from nyimplantdentistry.com

The distribution of energy from a fiber tip is highly dependent on the shape of the tip. Using ray tracing, the distribution of flat and tapered tips have previously been studied by Verdaasdonk et al. [7]. As shown in figure 4 and 5, the energy from the flat tip is emitted in a slightly divergent beam, whereas the beam from tapered tip is conical shaped irradiating to the side. The distribution is dependent on the angle of the taper on the fiber.

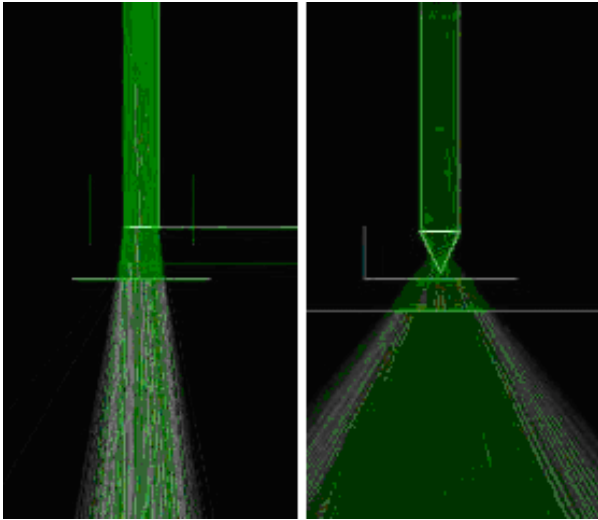


Figure 4. Ray tracing imaging of a flat tip (L) and a tapered tip (R). Adapted from [7]

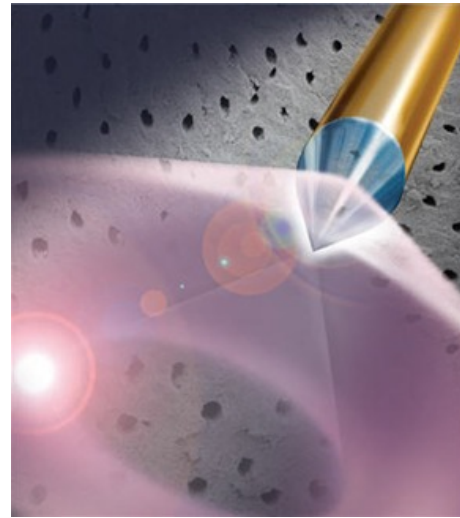


Figure 5. Artist impression of laser light emitted from a tapered tip. From [www.biolase.com](http://www.biolase.com)

### 3. METHODS AND MATERIALS

#### 3.1 Description of experiments

In this study, the dynamics of explosive bubble formation in water was investigated in relation to absorption at  $2.78 \mu\text{m}$  (Er,Cr;YSGG) and  $2.94 \mu\text{m}$  (Er:YAG), pulse length from 20 to  $150 \mu\text{s}$  and fiber tip shape. The fiber tips used are either flat or tapered at a  $55^\circ$  angle. To visualize the bubble formation process, the end of the laser tip was emerged in a container of water while a camera with close-up optics captured the process. The energy is typically delivered through a hollow waveguide to the dental hand piece and at the end transmitted through a silica tip with a diameter of 200, 300 or  $400 \mu\text{m}$  (Z2, Z3, Z4) and lengths from 9 mm to 33 mm. Various laser tips are shown in figure 6. The pulse energy was measured with an external energy meter.

Figure 6. Laser tips with varying lengths and diameters. Image from [www.biolase.com](http://www.biolase.com)



#### 3.2 High speed imaging setup

Vapor bubble formation and implosion are fast processes that evolve mainly in the range from microsecond to millisecond. Normally, a highly specialized and expensive camera system would be needed, capable of capturing a million frames per second, in order to visualize this process. However, in vitro under controlled conditions, experiments can be repeated and are reproducible. Therefore, an alternate high-speed imaging technique was applied in this study, as described by Verdaasdonk et al. [8] With this method, laser-water interaction is visualized by capturing images at preset

delays. For each individual laser pulse, one image is captured at a certain delay. By combining the images from multiple pulses, each with a increasing delay time, the entire bubble formation and cavitation process can be reconstructed.

At the onset of a laser pulse from either the Er,Cr:YSGG laser or the Er:YAG laser, a signal was sent through an amplifier and a programmed time-delay box to trigger a flash lamp. The light flash of 2  $\mu\text{s}$  was aimed at the target at a specific angle to obtain maximum contrast. At the same time, a CCD camera was triggered to capture the target with the time resolution of the flash. The delay box was programmed to extend the delay at each consequent laser pulse with preset steps of 10  $\mu\text{s}$ . A schematic representation of the setup is shown in figure 7.

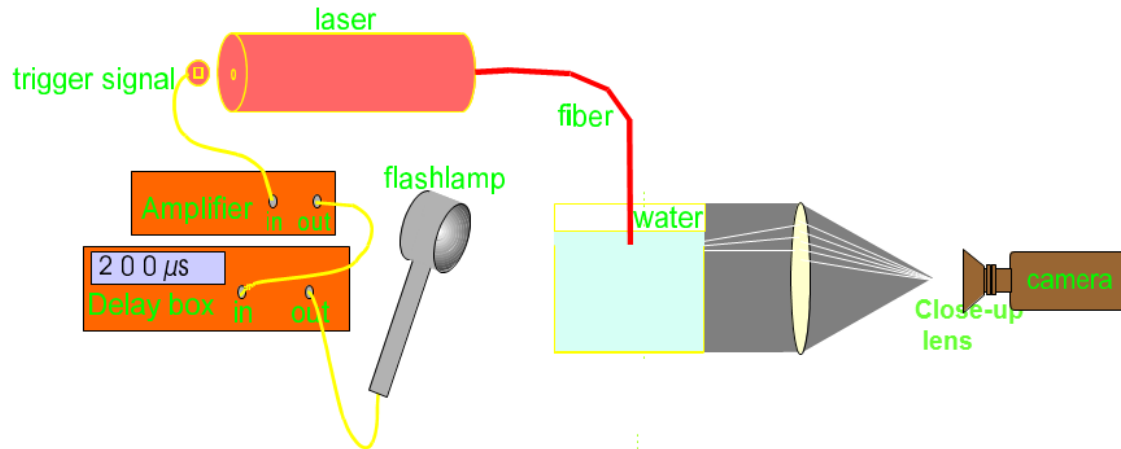


Figure 7. Schematic representation of the high speed time delayed flash imaging setup [8]

### 3.3 Parameters investigated

Using time delayed high speed  $\mu\text{s}$  flash imaging, sequences of the dynamics of exploding and imploding bubbles between 10 - 300  $\mu\text{s}$  are assembled for pulse energies from 10 to 50 mJ. The bubbles formed by Er:YAG and Er,Cr:YSGG lasers were compared in relation to pulse energy, pulse length and shape of the fiber tip, flat or tapered.

### 3.4 Data analysis

Frames captured with the high-speed imaging technique were combined to reconstruct a sequence of the expansion and implosion of the cavitation bubbles at the various parameters being studied. To characterize the bubble, the expansion and collapse is determined by measuring the length and width in relation to time(see figure 8).

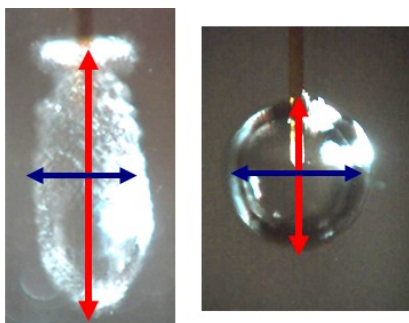


Figure 8. The length (red, vertical) and width (blue, horizontal) of the bubbles

## 4. RESULTS

### 4.1 Er,Cr:YSGG versus Er:YAG

There is no significant difference in bubble shape comparing 2.78 and 2.94  $\mu\text{m}$  lasers at the same settings. See figures 9 and 10. The size/shape of the bubbles, as well as the duration of the formation and implosion of the bubbles is virtually equal for the Er,Cr:YSGG and Er:YAG lasers independent of tip shape and size.



Figure 9. Flat tip.  
Left: Er:YAG, right: Er,Cr:YSGG.  
Both with an energy of 20 mJ, using a  
200  $\mu\text{m}$  in diameter tip, 50  $\mu\text{s}$  pulse



Figure 10. Tapered tip.  
Left: Er:YAG, right: Er,Cr:YSGG.  
Both with an energy of 20 mJ, using a  
200  $\mu\text{m}$  in diameter tip, 50  $\mu\text{s}$  pulse

### 4.2 Tapered tip versus flat tip

For a flat tip, the cavitation bubble appears as an elongated bubble with a diffuse surface. After around 100  $\mu\text{s}$ , the bubble will separate from the laser tip and implode. A sequence of video frames of the process of an expanding and imploding cavitation bubble, induced by a flat tip, is presented in figure 11. To quantify the dynamics of the shape of the bubble in relation to time, the length and width of the bubble are plotted against time in figure 12. During the expansion of the bubble, it is mainly the length of the bubble that increases. This results in a more elongated bubble shape.

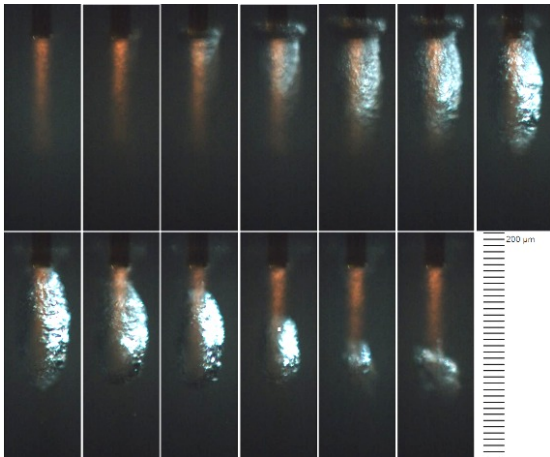


Figure 11. Video frames of an expanding and imploding cavitation bubble from 20 to 260  $\mu\text{s}$  after the onset of a 40 mJ Er:YAG laser pulse in an open space water environment. 400  $\mu\text{m}$  diameter flat tip

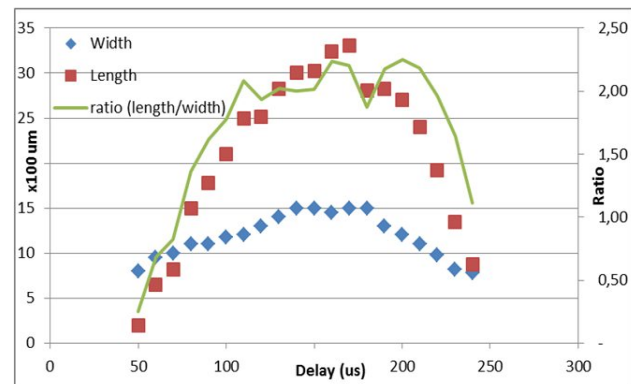


Figure 12. Graph of dynamics of bubble size in time for Er:YAG, 400  $\mu\text{m}$  diameter flat tip, pulse energy 40 mJ

In contrast to the flat tip, a tapered tip creates a spherical bubble, with an optically smooth surface. Video frames of the expanding and imploding cavitation bubble, induced by a tapered laser tip, are presented in figure 13.

To quantify the dynamics of the shape of the bubble in relation to time, the length and width of the bubble are plotted against time in figure 14.



Figure 13. Video frames of an expanding and imploding vapor bubble from 40 to 300  $\mu\text{s}$  after the onset of a 40 mJ Er:YAG laser pulse in an open space water environment. 400  $\mu\text{m}$  diameter tapered tip

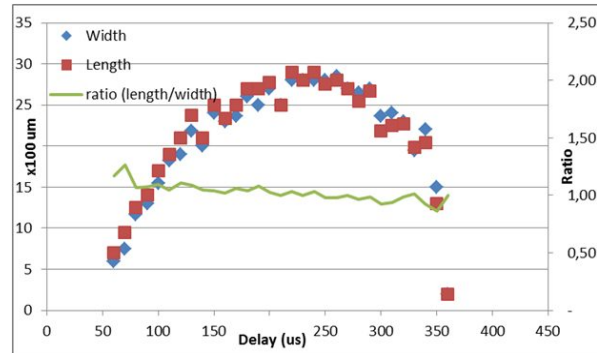


Figure 14. Graph of dynamics of bubble size in time for Er:YAG laser, 400  $\mu\text{m}$  diameter tapered tip. 40 mJ

The ratio between the length and width of the cavitation bubble induced by a tapered tip is close to 1 through the entire expansion and implosion process which is representative for a spherical bubble (figure 14).

A ring may form in the lower half of the bubble, due to the beam characteristics in the vapor environment within the bubble (figure 4). The duration of the bubble is comparable to the bubble formed using a flat tip, albeit the size may linger at its largest point, unlike the elongated bubble. The implosion of the spherical bubble is focused toward the fiber tip itself.

### 4.3 Pulse energy

Increasing the pulse energy results in larger bubble sizes. Both the time it takes for the bubble to reach its maximum size and the entire formation and implosion process is longer when the energy is increased.

Video frames of cavitation bubbles of a flat tip are presented in figure 15. The captured frames are chosen at the moment that the bubble reached its maximal size.

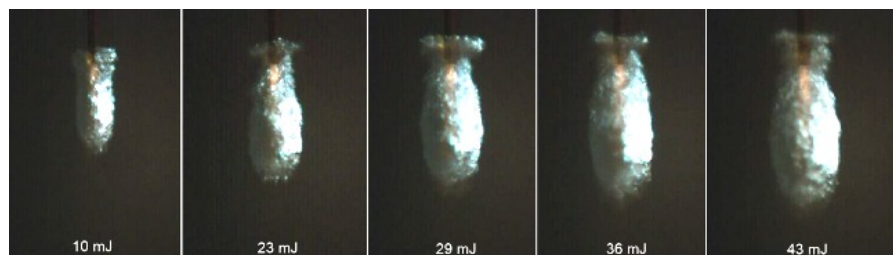


Figure 15. Flat tip, increasing energy 10 - 43 mJ, frames captured at the maximum size of the bubble

In figure 16 a graph is presented of four cavitation bubbles with all parameters identical except for the pulse energy.

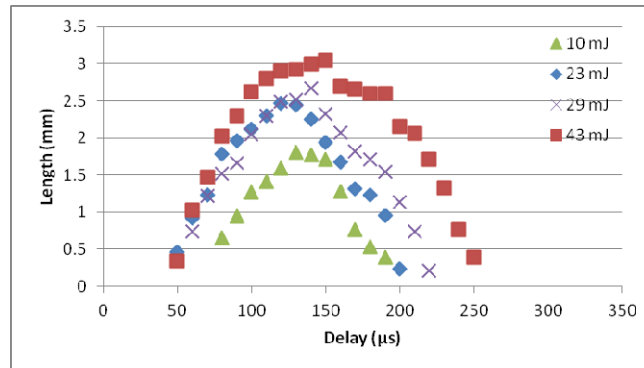


Figure 16. Graph of dynamics of bubble size in time for flat tip at 10, 23 29 and 43 mJ pulse energy, Er:YAG laser, 200 μm tip diameter

Video frames of cavitation bubbles of a tapered tip are presented in figure 17. The captured frames are chosen at the moment that the bubble reached its maximal size.

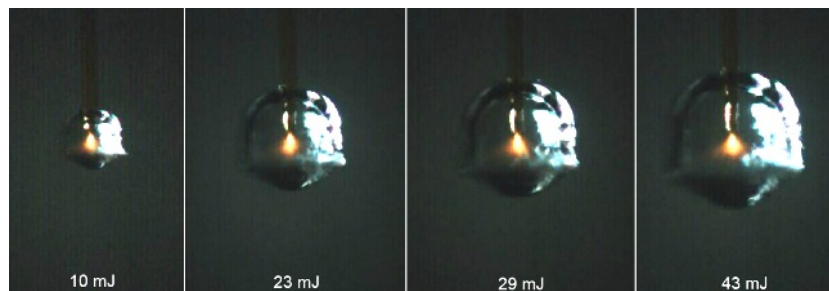


Figure 17. Tapered tip, increasing energy 10 - 43 mJ, frame captured at maximum size of bubble

In figure 18, a graph is presented of four cavitation bubbles with all parameters identical except for the pulse energy. The trend of longer bubble life time for a higher energy setting seems not consistent for the 43 mJ pulse with the tapered tip.

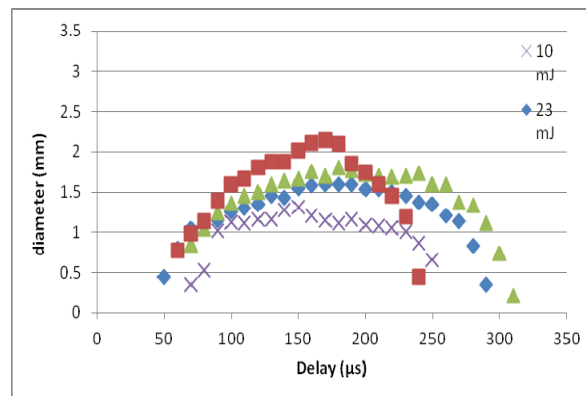


Figure 18. Graph of dynamics of bubble size in time for tapered tip, pulse energies 10, 23, 29 and 43 mJ, Er:YAG laser, 200 μm tip diameter,

#### 4.4 Different pulse lengths

Increasing the pulse duration of the laser with a flat tip creates bubbles with more elongated shape. The bubbles induced with a short pulse duration are more spherical in shape. The bubble shortens in length and becomes less wide as the pulse duration increases. Furthermore, the surface of the bubble will transform from smooth to a more diffuse appearance (see figure 19). The captured frames are chosen at the moment that the bubble reaches its maximal size.

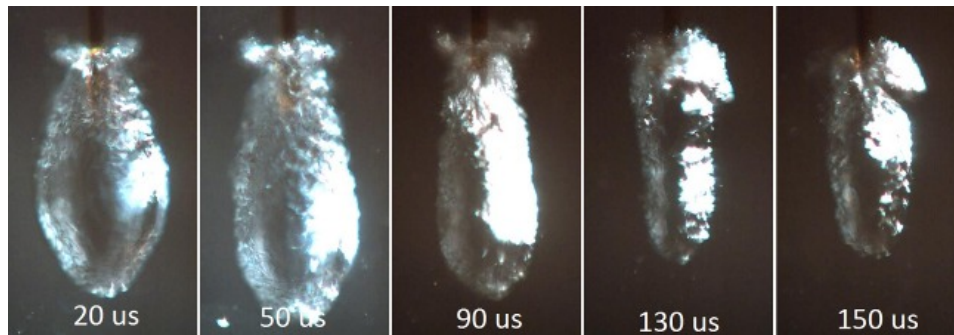


Figure 19. Er,Cr:YSGG laser, increasing pulse lengths (20  $\mu$ s – 150  $\mu$ s), flat tip (200  $\mu$ m), 20 mJ, at maximum size

A different result is observed with the tapered fiber tip. As the pulse duration is increased, a ring forms on the lower half of the bubble. There is no other difference in shape or size of the bubble (see figure 20). The captured frames are chosen at the moment that the bubble reaches its maximal size.

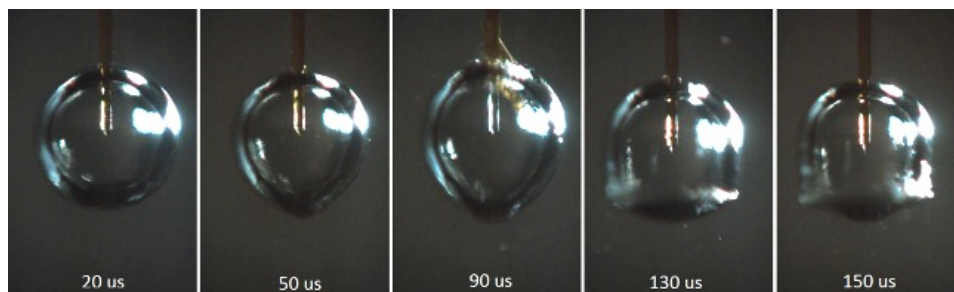


Figure 20. Er,Cr:YSGG laser, increasing pulse lengths (20  $\mu$ s – 150  $\mu$ s), tapered tip (200  $\mu$ m), 20 mJ, at maximum size

## 5. DISCUSSION

The aim of this study was to obtain a better understanding of the dynamics exploding and imploding vapor bubbles induced by Erbium laser systems in relation to wavelength, tip shapes, pulse length and energy levels.

### 5.1 Wavelength

Although the absorption 2.94  $\mu$ m Er:YAG laser is 3 times higher in water compared to the 2.78  $\mu$ m Er,Cr:YSGG laser the bubble size and shape are similar. For these high absorption levels, the laser energy is instantly absorbed in water at and vaporizations start at the beginning of the pulse making the effect of pulse length and total pulse energy more dominant for the bubble dynamics.

### 5.2 Tip shape

There is a clear difference in the shape and dynamics comparing the bubbles from a flat and tapered tip. When the initial layer of water at the fiber tip absorbs the laser energy, the high pressure vapor formed expands explosively in the direction perpendicular from the surface. For the flat tip in forward direction. Following the laser beam will emit through

the water vapor and continue to vaporize the far end of the bubble 'drilling a way through the water'. This phenomenon has been referred to as the 'Moses effect in the microsecond region' [9].

The tapered tip shape provide a larger total surface compared to a flat tip and when the vapor starts expanding explosively perpendicular to the surface. This is already in a dome shape and, due to surface tension, it easily expands further into a sphere. Following the laser beam will be directed in a cone shape through the vapor bubble as shown in figure 4 resulting in additional vaporization on the sides of the bubble as can be clearly appreciated in figure 20 for longer pulse lengths (120 and 150  $\mu$ s).

Due to the spherical shape the implosion of the bubble will be focused back in the center near the tip of the taper. This will results in high mechanical stress, microjets and shock waves. These forces can induce damage to the tip and the environment which can be intended (cutting hard tissue) or an adverse effect (e.g. breaking the fiber tip). The degradation of the fiber tip due to the dynamics of cavitation bubbles is illustrated in figure 21 [10]. In contrast, the bubbles induced by the flat fiber, seem to implode in a more gradual way, however, cavitation and microjets can still be expected.

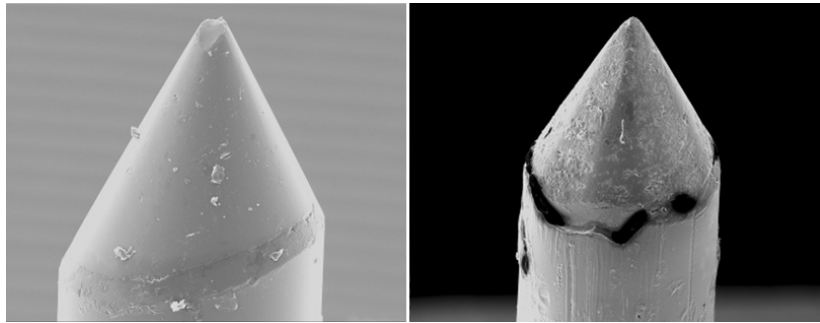


Figure 21. A tapered fiber tip before and after usage. Image from Verdaasdonk et al.[10]

### 5.3 Pulse length

When the laser energy is absorbed during a longer pulse length, the initial formation of vapor will be less forceful and heat conduction will spread the energy to a larger volume of water making the threshold of vaporization higher.

During the pulse the vapor already starts to condensate resulting in smaller bubbles. This is in accordance to previous findings by Mrochen et al. [11]. These effects can be appreciated especially in figure 19. The bubbles for the 20  $\mu$ s are more symmetric and smooth compared to the 150  $\mu$ s bubbles.

### 5.4 Pulse energy

As can be expected the bubbles grow to a larger diameter increasing the energy of the pulse (figures 15-18). Also the dynamic life time cycle of the bubble, expanding and imploding, increases with energy [9]. Although, there seems one exception for the tapered tip at 43 mJ (figure 18) which might be ascribed to a non-linear effect inducing a faster implosion or a deviation in experimental settings that could not be verified afterwards.

## 6. CONCLUSIONS AND IMPLICATIONS FOR DENTISTRY

The behavior of the explosive vapor bubbles and related cavitation effects were studied under water. This has provided insight and enabled comparison between the Erbium wavelengths and influence of pulse length, energy and tip shape. In dental practice, the Erbium lasers are mostly applied with a water spray for drilling. More representative for a water environment are the applications in gum pockets or inside the root canal. However, the dynamics of the bubbles in narrow area like the crown of a tooth or a root canal will be different as shown in a previous study [12].

Still, the basic findings that there is no difference in the bubble dynamics (hence ablation mechanism) between Er:YAG and Er,Cr:YSGG lasers and on the other hand the significant difference between flat and tapered tips, are important take home messages for future research

## REFERENCES

- [1] Niemz M., "*Laser-Tissue Interactions - Fundamentals and Applications*," Springer, (2007)
- [2] Shrivastava S.K. Kailash ., "*Shock wave treatment in medicine*," Journal of Biosciences 30, 269-275 (2005)
- [3] Koechner W., "*Solid-state laser engineering*," Springer New York, (2006)
- [4] Brennen C. E., "*Cavitation and Bubble Dynamics*," Oxford University Press, (1995)
- [5] Harrington J.A., "*Infrared Fibers and Their Applications*," SPIE Press Book, (2004)
- [6] Matsuura Y., Abel T., Harrington J.A., "*Optical properties of small-bore hollow glass waveguides*," Applied Optics 34, 6842-6847 (1995)
- [7] Verdaasdonk R.M., "*Medical applications of lasers*." In Advances in Lasers and Applications. Institute of Physics Publishing Bristol, 181-226 (1999)
- [8] Verdaasdonk R.M., van Swol C.F.P., Grimbergen M.C.M and Rem A.I., "*Imaging techniques for research and education of thermal and mechanical interactions of lasers with biological and model tissues*," Journal of Biomedical Optics 11, 041110 (2006)
- [9] Leeuwen T.G.J.M. van, Verdaasdonk R.M. and Borst C., "*Influence of holmium:YSGG intensity on bubble formation in saline and in tissue*," SPIE Vol 1646, 307-314 (1992)
- [10] Verdaasdonk, R.M., Klaessens, J, de Roode, R., de Boorder, T. and Blanken, J., "*Dynamic change of characteristics of (modified) fiber tips used with microsecond pulsed lasers in a liquid environment influencing the effectiveness and safety of treatment*." SPIE Vol 6435, (2007)
- [11] Mrochen M., Riedel P., Donitzky C., Seiler T., "*Zur Entstehung von Kavitationsblasen bei der Erbium:YAG-Laser-Vitrektomie*," Der Ophthalmologe 98, 163-167 (2001)
- [12] Blanken J, DeMoor R, Meire M, Verdaasdonk R. "*Laser induced explosive vapor and cavitation resulting in effective irrigation of the root canal. Part 1: a visualization study*." Lasers Surg Med 41, 514-519 (2009)